

Covariant Formulation of the Transition Radiation Energy Spectrum of an Electron Beam at a Normal Angle of Incidence onto a Round Metallic Screen

Gian Luca Orlandi

Paul Scherrer Institut, 5232 Villigen PSI, CH.

Abstract

In the transition radiation emission from a N electron bunch hitting at a normal angle of incidence a metallic screen, the transverse and the longitudinal spatial coordinates of the electron bunch play different roles in determining the N single electron radiation field amplitudes and their relative phases in relation to the different physical constraints which an electromagnetic radiative mechanism by a charged beam must meet: i.e., temporal causality and covariance. The distribution of the N electron longitudinal coordinates determines indeed the sequence of the N electron collisions onto the metallic screen and, on the basis of the temporal causality principle, it also determines the distribution function of the relative emission phases of the N single electron field amplitudes from the metallic surface. The distribution of the transverse coordinates of the N electrons contributes as well to determine the relative phase distribution of the N electron field amplitudes at the observation point - located on the longitudinal axis of the reference frame - providing a further phase information that accounts for the transverse displacement of the N electrons with respect to the beam axis. The distribution of the transverse coordinates of the N electrons is a relativistic invariant under a Lorentz transformation with respect to the direction of motion of the beam and, consequently, it is expected to leave a covariant mark on the N single electron amplitudes composing the radiation field. The covariant imprinting of the N electron transverse density on the radiation field affects both the temporal coherent and incoherent parts of the transition radiation

Email address: gianluca.orlandi@psi.ch (Gian Luca Orlandi)

energy spectrum. Such a dependence of the N single electron radiation field amplitudes on the electron density in the transverse plane manifests itself as an increase - towards an asymptotic limit - of the radiated spectral energy with the decrease of the beam transverse size and as a spectral narrowing of the angular distribution of the radiation intensity with respect to the ideal case of a single electron hitting an infinite metallic screen. In the case of a round metallic screen with an arbitrary radius, the formal expression of the transition radiation energy spectrum will be derived and numerical results will be presented.

Keywords: Form Factor, Coherence, Fourier Transform, Collective Effects
PACS: 41.60.-m, 41.75.-i, 42.25.Kb, 42.30.Kq

1 Introduction

2 A relativistic charge crossing a dielectric interface in a rectilinear and uni-
3 form motion can originate a highly directional and broad wavelength band
4 radiation emission propagating backward and forward from the boundary
5 surface within a small angle scaling down with the energy of the charge, the
6 so called transition radiation [1, 2, 3, 4, 5, 6, 7, 8, 9]. Thanks to the instan-
7 tantaneous, highly directional and charge-energy dependent features, transition
8 radiation is a precious tool in the beam diagnostics of a particle accelerator.
9 In the vacuum chamber of a particle accelerator the relativistic charged beam
10 can be indeed intercepted by a movable thin metallic screen and the resulting
11 light pulse can be imaged by a CCD-camera (Charge-Coupled-Device), for
12 instance, to measure the transverse profile of the charged beam. Under the
13 key-word OTR Beam Diagnostics (Optical Transition Radiation), the reader
14 can find an enormous specialized literature dedicated to this topic. For most
15 part of the practical detection conditions (from the extreme visible to the
16 THz region), the metallic screen can be assimilated to an ideal conductor
17 surface and the transition radiation emission can be easily schematized as
18 the result of the dipolar oscillation of the conduction electrons of the metal-
19 lic surface induced by the electromagnetic field of the incident relativistic
20 charge. The dipolar oscillation induced in the double layer of charge by the
21 relativistic charge explains indeed how an electromagnetic radiative mecha-
22 nism, originated by a charge in a rectilinear and uniform motion, can also
23 propagate in the backward direction. Such a model of the double layer of
24 charge, describing the transition radiation emission as the result of the dipo-

25 lar oscillation of the conduction electrons induced by the relativistic charge,
26 is also enlightening about the kinematics of this radiative mechanism and
27 about the common relativistic nature that it shares with other electromag-
28 netic radiative mechanisms by relativistic charged beams. The kinematics of
29 the transition radiative mechanism can be indeed schematized as the head-
30 on collision of two distributions of charge as observed in the reference frame
31 of rest of one of the two colliding charged distributions. The backward and
32 forward double conical transition radiation emission can be thus interpreted
33 as the photon bremsstrahlung emission that two head-on colliding electron
34 beams can originate. Taking into consideration that the transition radiation
35 mechanism shares with other electromagnetic radiative mechanisms, such
36 as the synchrotron or the bremsstrahlung radiation, the same kinematical
37 and relativistic nature, it is thus reasonable to expect that, even at a very
38 short wavelength, some spectral modifications of the radiation intensity due
39 to transverse density of the beam should also affect the transition radiative
40 mechanism by an electron beam in a similar way as, in other electromagnetic
41 radiative mechanism by charged beams, the beam transverse size contributes
42 to determine the so called Brilliance or Luminosity properties of the radiation
43 source.

44 In the case of an electron beam at a normal angle of incidence onto a
45 metallic screen with arbitrary size and shape, it can be demonstrated that
46 a covariant and temporal causal formulation of the transition radiation en-
47 ergy spectrum of an electron beam necessarily implies, even at a very short
48 wavelength, a dependence of the radiation spectral intensity on the distri-
49 bution function of the particle density in the transverse plane [10]. In fact,
50 in the transition radiation emission of an electron beam at a normal angle
51 of incidence onto a metallic screen, the longitudinal and transverse coordi-
52 nates of the electrons play different roles. The distribution function of the
53 longitudinal coordinates of the N electrons determines indeed the sequence
54 of the particle collisions onto the metallic screen and, consequently, on the
55 basis of the temporal causality principle, also the distribution function of the
56 relative emission phases - from the metallic surface - of the N single electron
57 amplitudes composing the radiation field. The distribution function of the
58 N electron transverse coordinates contributes as well in determining the re-
59 lative phase delay of the N single electron field amplitudes at the observa-
60 tion point as a function of the transverse displacement of the N electrons with
61 respect to the beam axis where the radiation field is supposed to be observed.
62 But, in addition, because of the relativistic invariance under a Lorentz trans-

63 formation in the direction of motion of the beam, the N electron transverse
64 density manifests itself as a covariant feature of the radiation field whose
65 observability can transform but not disappear under a Lorentz transforma-
66 tion. In the present work, the covariant and temporal causal formula of the
67 transition radiation energy spectrum of a N electron bunch, already derived
68 in an implicit form in [10] in the most general case of a radiator surface with
69 an arbitrary size and shape, will be here rendered into an explicit form in the
70 particular case of a round radiator with an arbitrary radius. The so obtained
71 formula of the transition radiation energy spectrum of a N electron bunch
72 at a normal angle of incidence onto a round metallic screen is demonstrated
73 to be temporal causal and covariant [10] and to reproduce, as a limit, some
74 results already well known in literature, such as: the Frank-Ginzburg formula
75 of the single particle transition radiation energy spectrum in the ideal case
76 of an infinite radiator or the single electron transition energy spectrum radi-
77 ated by a round metallic screen with a finite radius. Finally, because of the
78 covariant dependence of the radiation field on the transverse density of the
79 N electrons, it results that the distribution function of the N electron trans-
80 verse coordinates affects both the temporal coherent and incoherent parts of
81 the transition radiation energy spectrum. Even at a very short wavelength,
82 the effect of the N electron transverse density on the spectral distribution of
83 the radiation intensity manifests itself as an increase of the radiated energy
84 with the decrease of the beam transverse size and a spectral narrowing of the
85 angular distribution of the radiation intensity in comparison with the ideal
86 case of an electron beam having a point-like transverse extension. In the
87 following, in the case of a bunch of N electrons hitting the metallic screen at
88 a normal angle of incidence, details on the formula of the transition radiation
89 energy spectrum and numerical results will be presented.

90 **2. Transition radiation energy spectrum of a N electron bunch**

91 A bunch of N electrons in a rectilinear and uniform motion along the
92 z -axis of the laboratory reference frame is colliding, at a normal angle of
93 incidence, onto a flat ideal conductor surface S placed in the plane $z = 0$.
94 The N electrons are supposed to fly in vacuum with a common velocity
95 $\vec{w} = (0, 0, w)$. All the electrons are supposed to hit the metallic screen at a
96 normal angle of incidence. Effects of the angular divergence of the electron
97 beam on the radiation energy spectrum are not considered in the present
98 work. The radiator surface S has a round shape with a finite radius R . The

99 observation point of the radiation emission is on the z -axis at a distance D
100 from the screen much larger than the observed wavelength λ . The spatial
101 coordinates of the N electrons being $[\vec{\rho}_{0j} = (x_{0j}, y_{0j}), z_{0j}]$ with $j = 1, \dots, N$
102 at a given reference time $t = 0$ when the center of mass of the charged
103 distribution is crossing the boundary surface, the spectral component of the
104 radiation field resulting from the collision of the N relativistic electrons onto
105 the metallic screen reads, see [10, 11, 12, 13, 14, 15, 16],

$$E_{x,y}^{tr}(\vec{\kappa}, \omega) = \sum_{j=1}^N H_{x,y}(\vec{\kappa}, \omega, \vec{\rho}_{0j}) e^{-i(\omega/w)z_{0j}} \quad (1)$$

106 where, under the far-field approximation [7, 9, 17], the single electron con-
107 tribution to the radiation field can be calculated in the most general case of
108 a radiator surface S with an arbitrary shape and size (either infinite $S = \infty$
109 or finite $S < \infty$) as follows [10, 11, 12, 13, 14, 15, 16]:

$$H_{x,y}(\vec{\kappa}, \omega, \vec{\rho}_{0j}) = \frac{iek}{2\pi^2 Dw} \int_S d\vec{\rho} \int d\vec{\tau} \frac{\tau_{x,y} e^{-i\vec{\tau} \cdot \vec{\rho}_{0j}}}{\tau^2 + \alpha^2} e^{i(\vec{\tau} - \vec{\kappa}) \cdot \vec{\rho}}. \quad (2)$$

110 In previous Equation, $k = \omega/c = 2\pi/\lambda$ is the wave number, $\vec{\kappa} = (k_x, k_y) =$
111 $k \sin \theta (\cos \phi, \sin \phi)$ is the transverse component of the wave-vector, $\alpha = \frac{\omega}{w\gamma}$
112 (γ being the relativistic Lorentz factor) and the vector $\vec{\rho} = (x, y)$ represents
113 the integration variable on the surface S of the screen.

114 With reference to Eqs.(1,2), the transition radiation energy spectrum by a
115 N electron beam can be finally calculated as the flux of the Poynting vector,
116 see also [10]:

$$\frac{d^2 I}{d\Omega d\omega} = \frac{cD^2}{4\pi^2} \sum_{\mu=x,y} \left(\sum_{j=1}^N |H_{\mu,j}|^2 + \sum_{j,l(j \neq l)=1}^N e^{-i(\omega/w)(z_{0j} - z_{0l})} H_{\mu,j} H_{\mu,l}^* \right), \quad (3)$$

117 where $H_{\mu,j} = H_{x,y}(\vec{\kappa}, \omega, \vec{\rho}_{0j})$ with $\mu = x, y$, as defined in Eq.(2).

118 The formal expression of the radiation field and of the radiation energy
119 spectrum of the N electron bunch, as represented in Eqs.(1,2) and Eq.(3)
120 in the most general case of a flat radiator surface S with an arbitrary size
121 and shape, meets the constraints of the temporal causality and of the covari-
122 ance. The structure of the emission phases from the screen of the N single
123 electron field amplitudes composing the radiation field - see Eqs.(1,2) - is

indeed causally related to the temporal sequence of the N particle collision onto the metallic screen. Furthermore, with reference to [10], covariant or covariance consistent are all the formal steps which, from the expression of the electromagnetic field of the N electron bunch in the laboratory reference frame, leads to the radiation field - see Eqs.(1,2) - and to the radiation energy spectrum, see Eq(3). For further details about the covariant and the temporal causal formulation of the transition radiation emission from a N electron bunch - as described in Eqs.(1,2,3) - the reader is addressed to [10].

For the sake of ease, in order to proceed with the formal explicit derivation of the transition radiation energy spectrum in the case of a round radiator with a radius R , a polar angle representation is considered for the following vectors

$$\begin{cases} \vec{\tau} = \tau(\cos \eta, \sin \eta) \\ \vec{\xi}_j = (\vec{\rho} - \vec{\rho}_{0j}) = \xi_j(\cos \psi_j, \sin \psi_j) \end{cases}$$

where $\xi_j = \sqrt{\rho^2 + \rho_{0j}^2 - 2\vec{\rho} \cdot \vec{\rho}_{0j}}$ ($j = 1, \dots, N$), $\vec{\rho}_{0j} = (x_{0j}, y_{0j})$ and $\vec{\rho} = (x, y)$ with $0 < \rho < R$ being the vectors of the N electron transverse coordinates and the vector of the screen coordinates, respectively. Taking into account the following integral representation of the Bessel function of the first kind [18] (see also Eq.(17) in [19]):

$$\int_0^{2\pi} d\psi \begin{pmatrix} \cos \psi \\ \sin \psi \end{pmatrix} e^{iab \cos(\psi-\phi)} = 2\pi i \begin{pmatrix} \cos \phi \\ \sin \phi \end{pmatrix} J_1(ab) \quad (4)$$

in the limit of a round metallic surface with a radius R much longer than the average transverse size of the beam ($R \gg \langle \rho_{0j} \rangle, j = 1, \dots, N$) the integral that, in Eq.(2), determine the single electron field amplitude can be explicitly calculated:

$$\begin{aligned} & \int_S d\vec{\rho} \int d\vec{\tau} \frac{\tau_{x,y} e^{-i\vec{\tau} \cdot \vec{\rho}_{0j}}}{\tau^2 + \alpha^2} e^{i(\vec{\tau} - \vec{\kappa}) \cdot \vec{\rho}} = \\ & = \int_S d(\vec{\rho} - \vec{\rho}_{0j}) e^{-i\vec{\kappa} \cdot (\vec{\rho} - \vec{\rho}_{0j} + \vec{\rho}_{0j})} \int d\vec{\tau} \frac{\tau_{x,y} e^{i\vec{\tau} \cdot (\vec{\rho} - \vec{\rho}_{0j})}}{\tau^2 + \alpha^2} = \\ & = e^{-i\vec{\kappa} \cdot \vec{\rho}_{0j}} \int d\vec{\xi}_j e^{-i\vec{\kappa} \cdot \vec{\xi}_j} \int d\vec{\tau} \frac{\tau_{x,y} e^{i\vec{\tau} \cdot \vec{\xi}_j}}{\tau^2 + \alpha^2} = \\ & = e^{-i\vec{\kappa} \cdot \vec{\rho}_{0j}} \int d\vec{\xi}_j e^{-i\vec{\kappa} \cdot \vec{\xi}_j} \int \frac{d\eta d\tau \tau^2}{\tau^2 + \alpha^2} \begin{pmatrix} \cos \eta \\ \sin \eta \end{pmatrix} e^{i\tau \xi_j \cos(\eta - \psi_j)} = \end{aligned}$$

$$\begin{aligned}
&= (2\pi i) e^{-i\vec{\kappa}\cdot\vec{\rho}_{0j}} \int d\xi_j \xi_j d\psi_j \begin{pmatrix} \cos \psi_j \\ \sin \psi_j \end{pmatrix} e^{-i\kappa\xi_j \cos(\psi_j-\phi)} \int_0^\infty \frac{d\tau \tau^2 J_1(\tau\xi_j)}{\tau^2 + \alpha^2} = \\
&= (2\pi)^2 \alpha \begin{pmatrix} \cos \phi \\ \sin \phi \end{pmatrix} e^{-i\vec{\kappa}\cdot\vec{\rho}_{0j}} \int_{\rho_{0j}}^{R+\rho_{0j}} d\xi_j \xi_j K_1(\alpha\xi_j) J_1(\kappa\xi_j) = \quad (5) \\
&= (2\pi)^2 \begin{pmatrix} \cos \phi \\ \sin \phi \end{pmatrix} \frac{\kappa e^{-i\vec{\kappa}\cdot\vec{\rho}_{0j}}}{\kappa^2 + \alpha^2} [\rho_{0j}\Phi(\kappa, \alpha, \rho_{0j}) - (R + \rho_{0j})\Phi(\kappa, \alpha, R + \rho_{0j})]
\end{aligned}$$

145 with

$$\Phi(\kappa, \alpha, \rho_{0j}) = \alpha J_0(\kappa\rho_{0j})K_1(\alpha\rho_{0j}) + \frac{\alpha^2}{\kappa} J_1(\kappa\rho_{0j})K_0(\alpha\rho_{0j}) \quad (6)$$

146 and

$$\Phi(\kappa, \alpha, R + \rho_{0j}) = \alpha J_0[\kappa(R + \rho_{0j})]K_1[\alpha(R + \rho_{0j})] + \frac{\alpha^2}{\kappa} J_1[\kappa(R + \rho_{0j})]K_0[\alpha(R + \rho_{0j})] \quad (7)$$

147 where Eqs.(5,6,7) follows from Eq.(4) and from formulas 6.566(2), 6.521(4),
148 8.473(1) and 8.486(17) in [18].

149 In conclusion, with reference to Eqs.(5,6,7), the harmonic component of
150 the radiation field produced by a N electron bunch hitting a round radiator
151 surface with a finite radius R reads, see Eqs.(1,2),

$$\begin{aligned}
E_{x,y}^{tr}(\vec{\kappa}, \omega) &= \sum_{j=1}^N H_{x,y}(\vec{\kappa}, \omega, \vec{\rho}_{0j}) e^{-i(\omega/w)z_{0j}} = \sum_{j=1}^N \frac{2iek}{Dw} \frac{\kappa}{\kappa^2 + \alpha^2} e^{-i[(\omega/w)z_{0j} + \vec{\kappa}\cdot\vec{\rho}_{0j}]} \times \\
&\times \begin{pmatrix} \cos \phi \\ \sin \phi \end{pmatrix} [\rho_{0j}\Phi(\kappa, \alpha, \rho_{0j}) - (R + \rho_{0j})\Phi(\kappa, \alpha, R + \rho_{0j})], \quad (8)
\end{aligned}$$

152 where $\vec{\kappa} = (\kappa_x, \kappa_y) = k \sin \theta (\cos \phi, \sin \phi)$ is the transverse component of the
153 wave-vector ($k = 2\pi/\lambda$). In some special and relevant cases, the formula of
154 the transition radiation field given in Eqs.(6,7,8) reproduces as a limit some
155 results already well known in literature.

156 Case1. Single electron ($j = 1$) and ($\rho_{0j} = 0, R = \infty$): i.e., a single
157 electron moving on the z -axis ($x = y = 0$), where the observation point is
158 also located, in collision onto a radiator having an infinite surface. In the
159 limit $R \rightarrow \infty$ and $\rho_{0j} \rightarrow 0$, the functions defined in Eqs.(6,7) tend to the
160 following limit values:

$$\begin{cases} (R + \rho_{0j})\Phi(\kappa, \alpha, R + \rho_{0j}) \rightarrow 0 \\ \rho_{0j}\Phi(\kappa, \alpha, \rho_{0j}) \rightarrow 1 \end{cases}$$

161 Taking into account the limits above, the following expression of the single
 162 electron radiation field, see Eqs.(6,7,8), follows

$$E_{x,y}^{tr}(\vec{\kappa}, \omega) = \frac{2iek}{Dw} \frac{\kappa}{\kappa^2 + \alpha^2} \begin{pmatrix} \cos \phi \\ \sin \phi \end{pmatrix} \quad (9)$$

163 where $\kappa = k \sin \theta$. Finally, from the Equation above and Eq.(3), the well
 164 known result of the Frank-Ginzburg formula of the transition radiation en-
 165 ergy spectrum in the ideal case of a single electron hitting an infinite ideal
 166 conductor surface can be obtained [1, 2, 3, 4, 5, 6, 7, 8]:

$$\frac{d^2 I_e}{d\Omega d\omega} = \frac{(e\beta)^2}{\pi^2 c} \frac{\sin^2 \theta}{(1 - \beta^2 \cos^2 \theta)^2}. \quad (10)$$

167 Case 2. Single electron ($j = 1$) and ($\rho_{0j} = 0, R < \infty$): similar experi-
 168 mental situation as in previous case but finite radius of the radiator. With
 169 reference to the above reported limit of the expression in Eq.(6) for $\rho_{0j} \rightarrow 0$,
 170 the radiation field reads, see Eqs.(1,2,5,6,7),

$$E_{x,y}^{tr}(\vec{\kappa}, \omega) = \frac{2iek}{Dw} \frac{\kappa}{\kappa^2 + \alpha^2} \begin{pmatrix} \cos \phi \\ \sin \phi \end{pmatrix} \left[1 - \alpha R J_0(\kappa R) K_1(\alpha R) - \frac{\alpha^2 R}{\kappa} J_1(\kappa R) K_0(\alpha R) \right] \quad (11)$$

171 which, in the far-field approximation, represents the radiation field of a single
 172 electron hitting a finite round metallic screen. In the case of a single elec-
 173 tron hitting a round metallic screen with a finite radius, as a function of the
 174 transverse extension ($\gamma\lambda/2\pi$) of the single electron virtual quanta field com-
 175 pared to the finite radius R of the radiator, the transition radiation energy
 176 spectrum experiences a low frequency diffractive cut-off. This problem was
 177 already tackled in several works [20, 21, 22, 23, 24, 25]. Compare Eq.(11) in
 178 the present work with Eqs.(8, 9) in [25], for instance.

179 Finally, from Eqs.(3,8), the explicit expression of the transition radiation
 180 energy spectrum of a N electron bunch colliding onto a round ideal conductor
 181 surface with a finite radius R can be obtained

$$\frac{d^2 I}{d\Omega d\omega} = \frac{d^2 I_e}{d\Omega d\omega} \left(\sum_{j=1}^N |A_j|^2 + \sum_{j,l(j \neq l)=1}^N A_j A_l^* e^{-i[(\omega/w)(z_{0j} - z_{0l}) + \vec{\kappa} \cdot (\vec{\rho}_{0j} - \vec{\rho}_{0l})]} \right) \quad (12)$$

182 where $\frac{d^2 I_e}{d\Omega d\omega}$ is the single electron radiation energy spectrum already defined
 183 in Eq.(10) and

$$A_j = \rho_{0j} \Phi(\kappa, \alpha, \rho_{0j}) - (R + \rho_{0j}) \Phi(\kappa, \alpha, R + \rho_{0j}) \simeq \rho_{0j} \Phi(\kappa, \alpha, \rho_{0j}), \quad (13)$$

184 the approximation in Eq.(13) being valid for most of the experimental sit-
185 uations where diffractive modifications of the spectral distribution of the
186 radiated energy due to the finite size of the screen can be neglected.

187 In the formula of the transition radiation energy spectrum of a N electron
188 beam, as explicitly derived in Eqs.(12,13) in the case of a normal collision
189 onto a round metallic screen with a finite radius R , the double role played
190 by the transverse coordinates of the N electrons appears evident. On the
191 one hand, as a function of the displacement of the electrons with respect
192 to the beam axis where the radiation field is supposed to be observed, they
193 contribute to determine the relative phase delay of the N electron field am-
194 plitudes at the observation point as the presence of the well known three-
195 dimensional phase factor in the temporal coherent part of the formula given
196 in Eq.(12) clearly indicates. On the other hand, because of the invariance
197 of the transverse density of the N electrons under a Lorentz transformation
198 in the direction of motion of the beam, the N single electron radiation field
199 amplitudes show a covariant dependence on the transverse density of the N
200 electron beam. As a result, see Eqs.(12,13), both the temporal coherent and
201 the temporal incoherent components of the transition radiation energy spec-
202 trum of a N electron beam differ from the ideal scenario of a single electron
203 hitting an infinite metallic screen. It results indeed that, even at a very short
204 wavelength, the radiation spectral intensity increases with the decrease of
205 the beam transverse size towards an asymptotic limit as well as the spec-
206 tral angular distribution of the radiation experiences a broadening towards
207 the asymptotic limit given by the well known ideal case of a single electron
208 hitting an infinite metallic surface.

209 In Figs.(1,2,3,4), results of the numerical simulation of the temporal in-
210 coherent part of the transition radiation spectrum produced by a gaussian
211 electron bunch with a transverse size much shorter than the finite radius of
212 the radiator are shown, see Eqs.(12,13). In Fig.(1), for a beam energy of
213 $500MeV$ and a bunch of $N = 10^5$ electrons, the angular distribution of the
214 transition radiation intensity in the visible (Green, $\lambda = 530nm$) for different
215 values of the beam standard deviation $\sigma = 10, 50, 100 \mu m$ is calculated and
216 compared with the ideal result obtainable from a bunch with the same charge
217 but radiating according to the formula given in Eq.(10). In Figs.(2,3,4), for
218 different beam energies $500, 750, 1000 MeV$ and a constant beam charge of
219 $N = 10^5$ electrons, the angular distributions of the transition radiation in-
220 tensity radiated at different wavelengths in the visible (Red, Green, Blue
221 $\lambda = 680, 530, 400 nm$) by a beam with standard deviation $\sigma = 50 \mu m$ are

222 compared with the analogous result obtained in the ideal case from the for-
223 mula in Eq.(10).

224 **3. Conclusions**

225 Temporal causality and covariance constrain the role that the distribu-
226 tions of the longitudinal and transverse coordinates of an electron bunch plays
227 in determining the physical features of an electromagnetic radiative mecha-
228 nism, in particular, the transition radiation mechanism. In the case of a N
229 electron bunch hitting at a normal angle of incidence a metallic screen, the
230 distribution of the electron longitudinal coordinates defines the causal corre-
231 lation occurring between the temporal sequence of the electron collisions onto
232 the metallic screen and the structure of the relative emission phases of the
233 N single electron radiation field amplitudes propagating from the metallic
234 screen to the observation point, located on the beam longitudinal axis. The
235 distribution of the transverse coordinates of the N electrons contributes as
236 well to determine the relative phase delay of the N single electron radiation
237 field amplitudes at the observation point as a function of the N electron
238 displacements with respect to the beam axis. The transverse density of the
239 N electrons, being an invariant under a Lorentz transformation with respect
240 to the direction of motion of the beam, constitutes for the radiation field
241 a covariant feature that affects both the spectral intensity and the angular
242 distributions of the transition radiation under observation conditions of both
243 temporal incoherence and temporal coherence. Compared to the reference
244 asymptotic results provided by the well known ideal formalism of a single
245 electron hitting an infinite metallic screen, an increase of the radiated spec-
246 tral intensity with the decrease of the beam transverse size and a broadening
247 of the spectral angular distribution constitute the relevant phenomenological
248 aspects of the covariant beam-transverse-size effects on the transition radia-
249 tion energy spectrum originated by an electron beam hitting a round metallic
250 screen at a normal angle of incidence.

251 **References**

- 252 [1] V. L. Ginzburg and I. M. Frank, Soviet Phys. JETP **16** (1946) 15.
253 [2] G.M. Garibian, Sov. Phys. JETP, **6** (33), 6 (1958) 1079-1085.
254 [3] G.M. Garibyan, Sov. Phys. JETP, **37** (10), 2 (1960) 372-376.

- 255 [4] I.M. Frank, Sov. Phys. Usp., **4**, 5, (1962) 740-746.
- 256 [5] F.G. Bass, V. M. Yakovenko, Sov. Phys. Usp., **8**, 3 (1965) 420-444.
- 257 [6] I.M. Frank, Sov. Phys. Usp., **8**, 5 (1966) 729-741.
- 258 [7] M.L. Ter-Mikaelian, *High-Energy Electromagnetic Processes in Con-*
259 *densed Media*, Wiley, New York (1972).
- 260 [8] V.L. Ginzburg, V.N. Tsytovich, *Transition Radiation and Transition*
261 *Scattering*, Adam Hilger, Bristol (1990).
- 262 [9] J.D. Jackson, *Classical Electrodynamics*, Wiley, New York (1975).
- 263 [10] G.L. Orlandi, *On the covariance of the charge form factor in the tran-*
264 *sition radiation energy spectrum of a beam at normal incidence onto a*
265 *metallic screen*, Paul Scherrer Institut Preprint PSI-PR-12-03.
- 266 [11] G.L. Orlandi, Opt. Commun. **211** (2002) 109-119.
- 267 [12] G.L. Orlandi, Opt. Commun. **267** (2006) 322-334.
- 268 [13] G.L. Orlandi, Proc. FEL 2005, Stanford University (2005), JACoW /
269 eConf C0508213, 576-579.
- 270 [14] G.L. Orlandi, Proc. EPAC 08, Genoa, Italy, (2008) 1221-1223.
- 271 [15] G.L. Orlandi, B. Beutner, R. Ischebeck, V. Schlott, B. Steffen, Proc.
272 FEL 2009, Liverpool, UK, 153 (2009).
- 273 [16] G.L. Orlandi, R. Ischebeck, V. Schlott, B. Steffen, Proc. FEL 2010,
274 Malmö, Sweden, (2010).
- 275 [17] M. Born, E. Wolf, *Principles of Optics*, Pergamon Press, Oxford (1965).
- 276 [18] I.S. Gradshteyn and I.M. Ryzhik, *Table of Integrals, Series, and Prod-*
277 *ucts*, 5th Ed. (1998) Academic Press.
- 278 [19] M. Castellano and V.A. Verzilov, Phys. Rev. ST-AB **1**, 062801 (1998).
- 279 [20] N.F. Shul'ga, S.N. Dobrovolsky, JETP Lett., Vol. **65**, No. 8, (1997)
280 611-614.

- 281 [21] A.P. Potylitsyn, Nucl. Instr. and Meth. in Phys. Res. B **145** (1998)
282 169-179.
- 283 [22] M. Castellano, A. Cianchi, G. Orlandi, V.A. Verzilov, Nucl. Instr. and
284 Meth. in Phys. Res. A **435** (1999) 297-307.
- 285 [23] S. Casalbuoni, B. Schmidt and P. Schmüser, TESLA Report 2005-15
286 (2005).
- 287 [24] D. Sütterlin, D. Erni, M. Dehler, H. Jäckel, H. Sigg, V. Schlott, Nucl.
288 Instr. and Meth. in Phys. Res. B **264** (2007) 361-370.
- 289 [25] S. Casalbuoni, B. Schmidt, P. Schmüser, V. Arsov, S. Wesch, Phys. Rev.
290 ST-AB **12**, 030705 (2009).

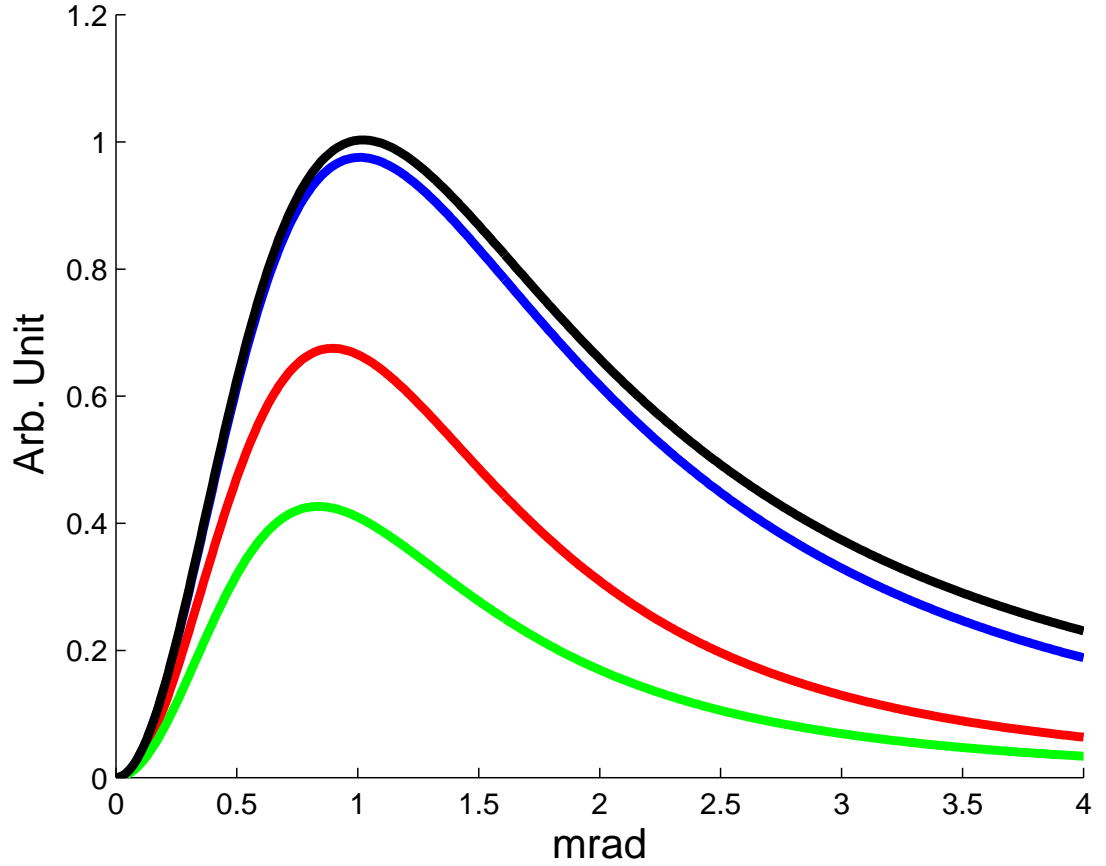


Figure 1: Angular distribution of the transition radiation emitted at a wavelength $\lambda = 530$ nm by a gaussian bunch of $N = 10^5$ electrons and energy 500 MeV with standard deviation $\sigma = 10$ μm (Blue curve), $\sigma = 50$ μm (Red curve) and $\sigma = 100$ μm (Green curve). The Blue, Red and Green curves are calculated via Eqs.(12,13) and compared with the analogous result (Black curve) that can be calculated in the same conditions of beam energy and charge via Eq.(10).

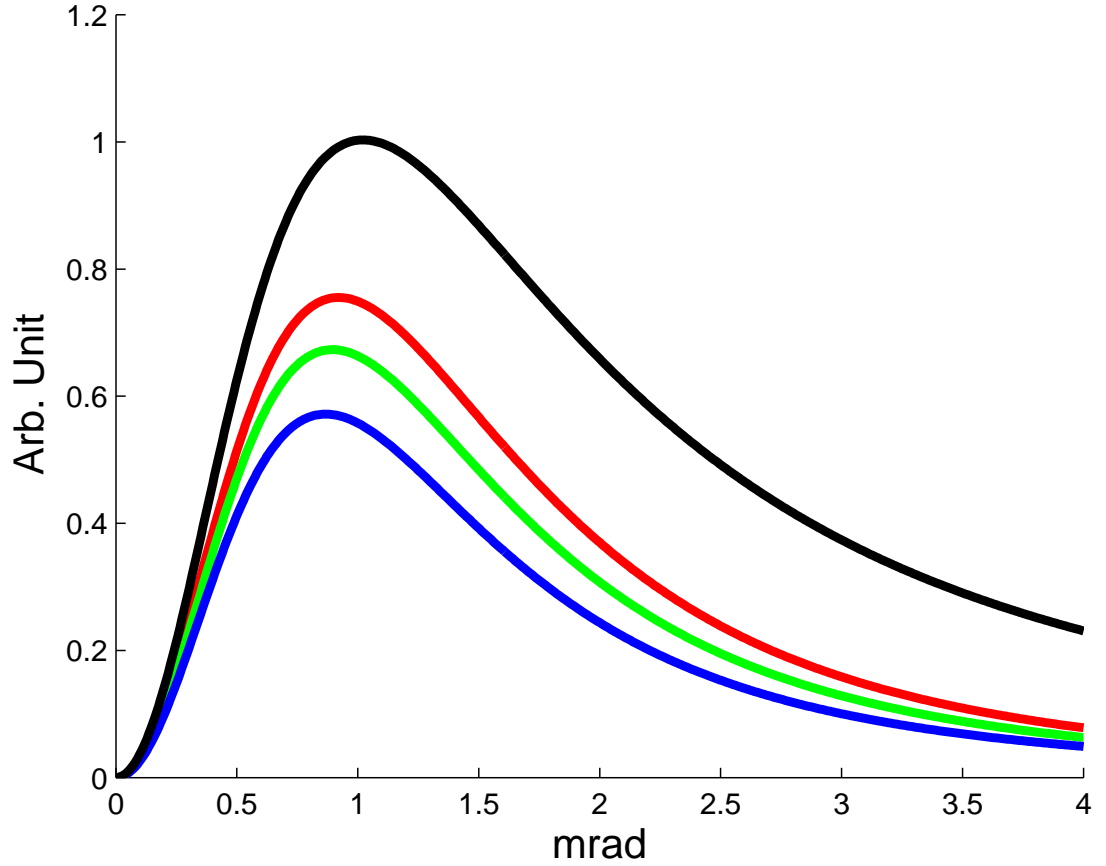


Figure 2: Beam energy 500 MeV . Angular distribution of the transition radiation emitted at a wavelength $\lambda = 680 \text{ nm}$ (Red curve), $\lambda = 530 \text{ nm}$ (Green curve), $\lambda = 400 \text{ nm}$ (Blue curve) by a gaussian bunch of $N = 10^5$ electrons with standard deviation $\sigma = 50 \text{ }\mu\text{m}$. The Blue, Red and Green curves are calculated via Eqs.(12,13) and compared with the analogous result (Black curve) that can be calculated in the same conditions of beam energy and charge via Eq.(10).

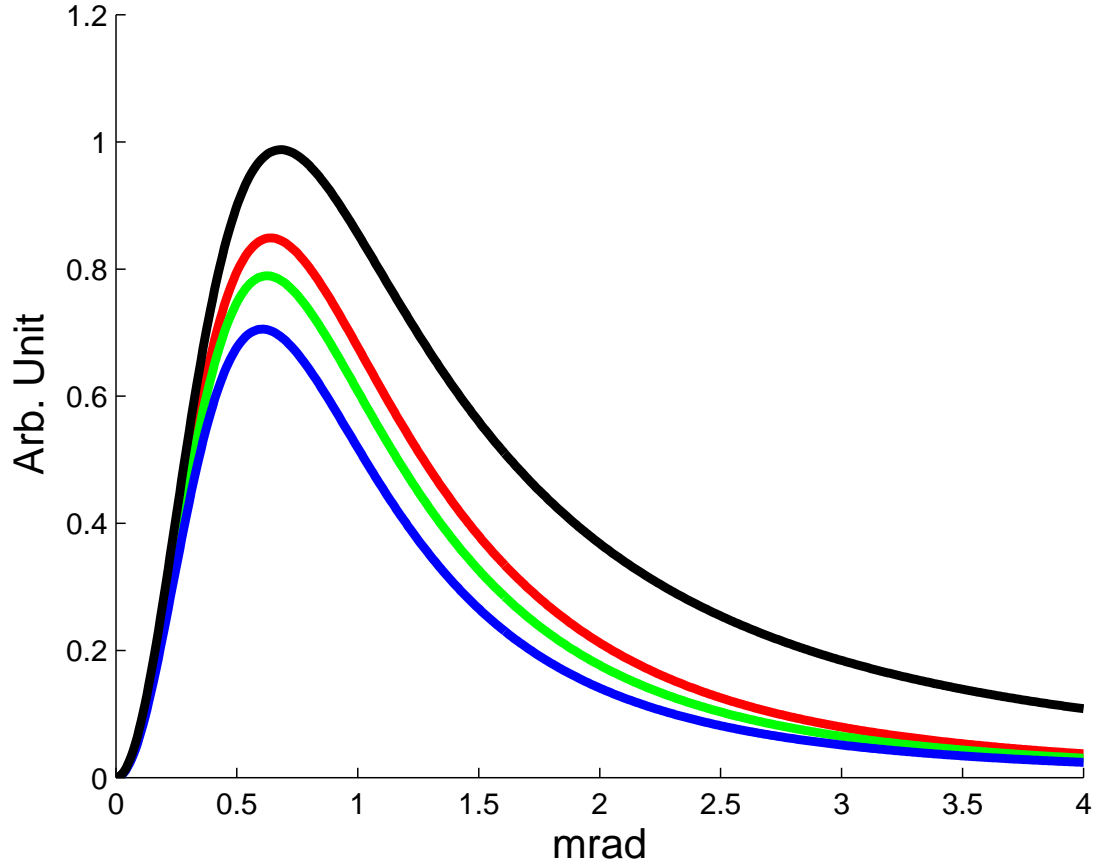


Figure 3: Beam energy 750 MeV . Angular distribution of the transition radiation emitted at a wavelength $\lambda = 680 \text{ nm}$ (Red curve), $\lambda = 530 \text{ nm}$ (Green curve), $\lambda = 400 \text{ nm}$ (Blue curve) by a gaussian bunch of $N = 10^5$ electrons with standard deviation $\sigma = 50 \text{ }\mu\text{m}$. The Blue, Red and Green curves are calculated via Eqs.(12,13) and compared with the analogous result (Black curve) that can be calculated in the same conditions of beam energy and charge via Eq.(10).

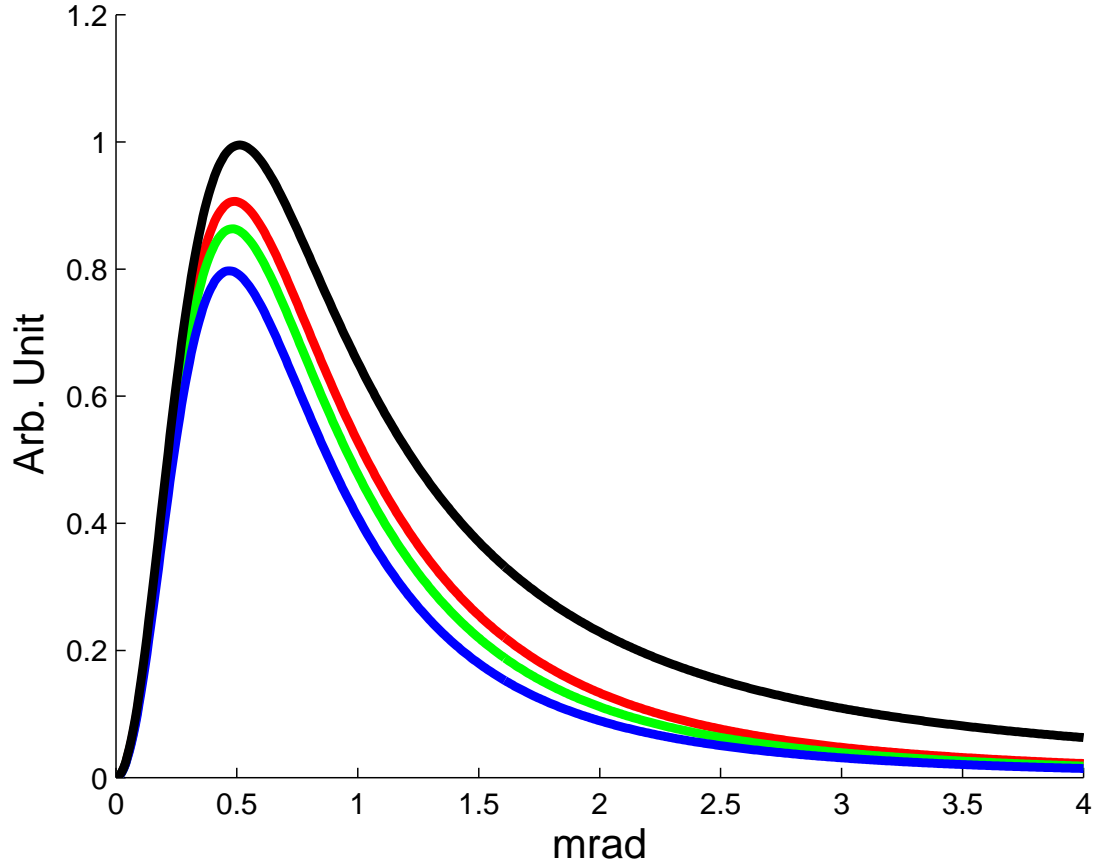


Figure 4: Beam energy 1000 MeV . Angular distribution of the transition radiation emitted at a wavelength $\lambda = 680 \text{ nm}$ (Red curve), $\lambda = 530 \text{ nm}$ (Green curve), $\lambda = 400 \text{ nm}$ (Blue curve) by a gaussian bunch of $N = 10^5$ electrons with standard deviation $\sigma = 50 \text{ }\mu\text{m}$. The Blue, Red and Green curves are calculated via Eqs.(12,13) and compared with the analogous result (Black curve) that can be calculated in the same conditions of beam energy and charge via Eq.(10).